JACS
JOURNAL OF THE AMERICAN CHEMICAL SOCIETY

Communication

pubs.acs.org/JACS

Plasmonically Nanoconfined Light Probing Invisible Phonon Modes in Defect-Free Graphene

Katsuyoshi Ikeda,*[,†,‡,§] Mai Takase,[†] Norihiko Hayazawa,[§,∥] Satoshi Kawata,[§,⊥] Kei Murakoshi,[†] and Kohei Uosaki[†,¶]

[†]Division of Chemistry, Graduate School of Science, Hokkaido University, Sapporo 060-0810, Japan

[‡]JST-PRESTO, Kawaguchi, Saitama 332-0012, Japan

[§]RIKEN, Wako, Saitama 351-0198, Japan

[∥]Department of Electronic Chemistry, Interdisciplinary Graduate School of Science and Engineering, Tokyo Institute of Technology, Yokohama, Kanagawa 226-8502, Japan

[⊥]Department of Applied Physics, Osaka University, Suita, Osaka 565-0871, Japan

[¶]International Center for Materials Nanoarchitechtonics (WPI-MANA), National Institute for Materials Science (NIMS), Tsukuba 305-0044, Japan

ABSTRACT: We present a simple plasmonic method that enables tuning of accessibility to the dipole-forbidden transition states of matter. This technique is realized by well-controlled plasmonic dimers, which can confine optical fields on the order of molecular dimensions. As an example, the approach is applied to activate *invisible* noncenter phonon modes of defect-free graphene in resonance Raman spectra. The relative intensity of the normally forbidden modes with respect to the dipole allowed modes progressively increases as the degree of field confinement increases. This opens up a novel avenue for both photochemical excitation of molecular systems and nanoscale characterization of materials.

Plasmonic manipulation of optical waves is a promising method to realize spatial focusing of optical fields beyond the diffraction limit.[1,2] This can result in both enhancement of local fields and generation of field gradients. The former effect has already been exploited to enhance light-matter interaction efficiency, such as surface enhanced Raman scattering (SERS)[3−5] or plasmon assisted photocurrent generation.[6,7] On the other hand, the latter contribution has not yet been utilized in practical research and applications, despite early reports on gradient field-induced SERS.[8,9] For the use of field gradients, a number of serious issues remain. The degree of optical field confinement needs to be controlled on the order of molecular dimensions ranging from a few ångstroms to several dozen ångstroms. Because the plasmonic field localization strongly depends on the size and shape of metal nanostructures,[10] this has not been trivial even in the recent nanotechnology. The position of target molecules with respect to the local fields is hardly controllable on a metal surface, which is also an essential factor that affects the degree of the gradient field contribution. Moreover, chemical interactions between target molecules and metal nanostructures are unavoidable, which may hinder the intrinsic effect of the field gradients.[11−13] In this communication, we demonstrate that tuning of the field gradients can control probability of originally forbidden nonvertical optical transitions in resonance SERS of defect-free graphene. The degree of field gradients is controlled by the gap size of metal nanodimers. The effect of the field gradients progressively increases as the gap size decreases, indicating that breaking of the dipole selection rules is plasmonically controllable.

Figure 1a shows the energy diagram for plasmon resonances of a pair of nanoparticles, which is widely recognized as a good model for realizing nanoconfined electric fields.[14] When these nanoparticles are nearly touching each other, four possible hybridized plasmon modes are built, as expected from the coupled dipole−dipole model.[15] Among these modes, the σ-mode is excited by linearly polarized light along the dimer axis, as a result of longitudinal coupling between the particle plasmons. The π^*-mode is excited due to transverse coupling when the polarization is perpendicular to the dimer axis. The remaining nonpolar σ^*- and π-modes are optically silent. The degree of field confinement for the σ-mode is controllable by varying the gap size of the dimer, d. In the present work, gold nanodimer arrays, as shown in Figure 1b, were fabricated on a glass substrate using double-angle evaporation of thin gold films with thickness of 30 nm though a shadow mask of a self-assembled monolayer of polystyrene beads.[16] In this technique, the nanoscale gap size, d, is adjusted by varying the evaporation angle of gold. Figure 1c shows the extinction spectra of a series of dimer arrays fabricated with slightly different evaporation angles around 11° normal to the substrate; the spectra are arranged in the order of decreasing d from (A) to (E). In sample (A) with the largest gap, the σ- and π^*-modes are seen around 820 and 730 nm, respectively. With decreasing d from (A) to (C), the σ-mode is gradually red-shifted while the π^*-mode is blue-shifted, in agreement with the coupled dipole−dipole model. For the much shorter gaps in samples (D) and (E), the plasmon resonance peaks were shifted in the opposite direction, which is explained by the quantum tunneling effect.[17,18] This typically occurs when the gap size is less than 1 nm. Hence, this result shows that the gap size is well-

Received: June 6, 2013
Published: July 19, 2013

dx.doi.org/10.1021/ja4056596 | J. Am. Chem. Soc. 2013, 135, 11489−11492

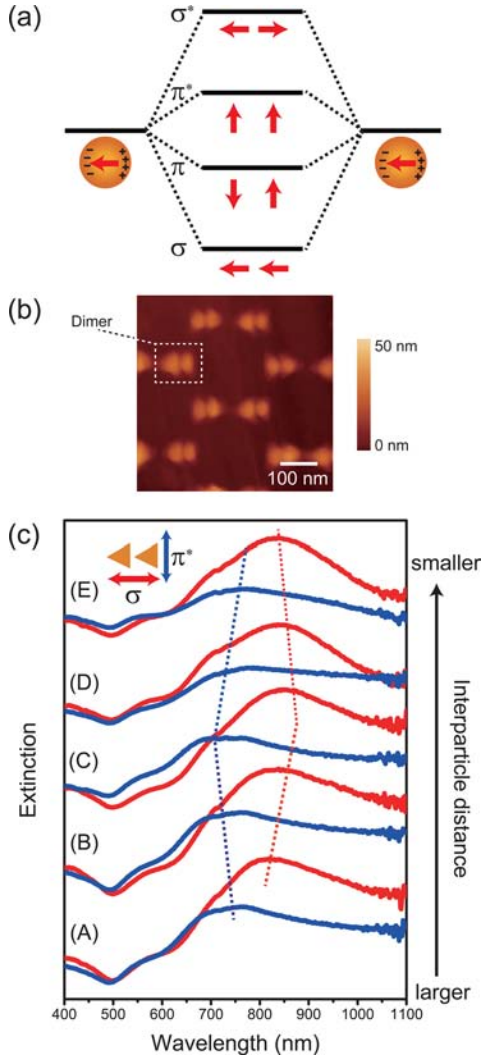

Figure 1. (a) Schematic illustration of the coupled dipole−dipole model of four possible hybridized plasmon modes in a metal nanodimer. (b) AFM image of a typical gold nanodimer array on a glass. (c) Dependence of plasmon resonances in the dimer system on the gap size and polarization.

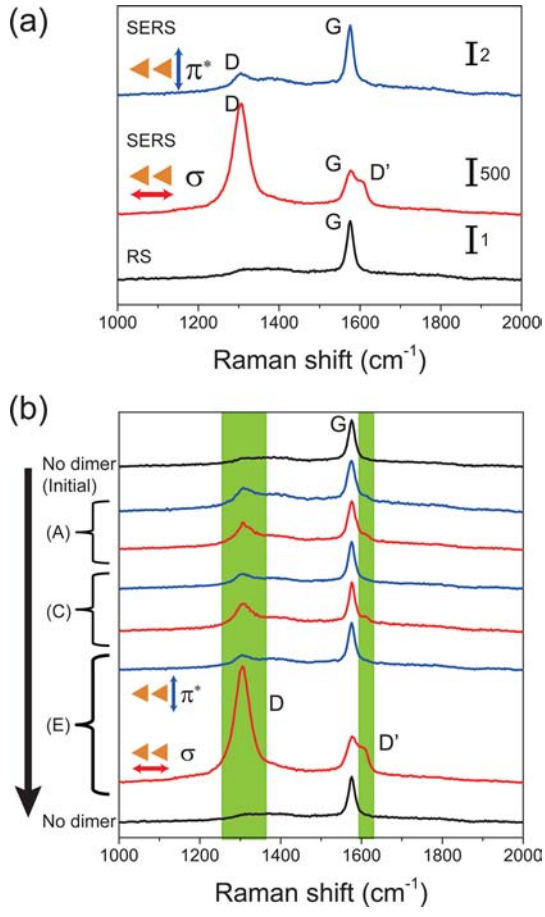

Figure 2. (a) Comparison of normal Raman and SERS spectra of defect-free graphene, measured by 785-nm excitation. For SERS, the dimer array (E) was attached to the graphene. (b) Dependence of the appearance of SERS spectra on the degree of field confinement, measured on the same graphene sample by alternating the dimer array step-by-step from (A) to (E).

controlled on the subnanometer order in the present system. The actual distance cannot be measured by AFM.

Graphene is suitable as a model to be placed strategically on plasmonic nanodimers, which is of great importance to examine the gradient field contribution, because of its micrometric size and very uniform structure. Graphene sheets of few layers were fabricated on a glass substrate using the "Scotch-tape" method. The thickness of the graphene was estimated to be $\lesssim$5 nm from AFM measurements. The quality of the sample was checked by Raman microscopy (Renishaw Ramascope, 100× objective, 785-nm excitation). After the measurement position was fixed at the defect-free area of the graphene, the other cover glass with a gold nanodimer array was attached on the top of the sample under microscope observation. Then, the SERS spectrum was taken at the same position to examine the field confinement effect.

Figure 2a shows conventional Raman and SERS spectra of the same few-layer graphene with and without the gold dimer array (E). The conventional Raman spectrum without the array only shows the Raman-active G-band at 1580 cm^{-1}, which is due to G-phonons near the Γ point of the Brillouin zone.[19] The absence of D- and D′-bands in the spectrum indicates that this graphene piece is defect-free, because these noncenter phonon modes, which are invisible under the electric dipole condition, are known to be activated by lattice defects.[20,21] In the presence of the gold dimer array, however, these originally Raman-forbidden D- and D′-bands were clearly seen at 1300 and 1620 cm^{-1}, respectively. The peak intensity of these bands was much larger for the σ-plasmon excitation than that for the π*-excitation, suggesting that the appearance of these bands is related to the plasmonic field localization. This is confirmed by measuring SERS for various gap sizes, d. Figure 2b shows normal Raman and SERS spectra of the same graphene, measured step-by-step by alternating the gold dimer arrays from (A) to (E); each spectrum is normalized with respect to the G-band intensity. Since the normal Raman spectra showed no D-band before and after the SERS measurements, it was confirmed that no detectable defects were induced during the experiment. For the SERS spectra, the σ-plasmon excitation always induced larger D- and D′-bands, compared with the π*-plasmon excitation. Importantly, the intensity of these bands under the σ-plasmon excitation was clearly dependent on d. That is, the normally forbidden Raman bands progressively increased in intensity as the gap size decreased. If the activation of these bands was due to chemical contributions through direct contact between graphene and the dimers, the relative

dx.doi.org/10.1021/ja4056596 | J. Am. Chem. Soc. 2013, 135, 11489−11492

peak intensity should not be dependent on d. Therefore, one can conclude that these modes were induced by the breaking of the dipole approximation condition through the field gradients.

The contribution of field gradients is also confirmed by tip-enhanced Raman spectroscopy (TERS). For the TERS measurements, an Ag-coated AFM tip was utilized as a plasmonic nanostructure, and 532-nm radiation was focused on it to generate nanoconfined fields.[22] Figure 3a shows a comparison between the topographic and TERS images for the G- and D-bands. In this nanoresolved image, the D-band is homogeneously seen over the entire sample area in the topograpy. Figure 3b shows a comparison of the spectra without and with tip enhancement, measured at the red-marked area. When the tip was far from the graphene surface, the Raman spectrum showed only the G-band. On the other hand, when the tip was very close to the surface, both the D- and D′-bands were induced in the spectrum. The G/D ratio is generally considered to be a quality parameter when carbon nanomaterials are characterized by Raman spectroscopy. Clearly, this is not valid in plasmonic nanoscale characterization.

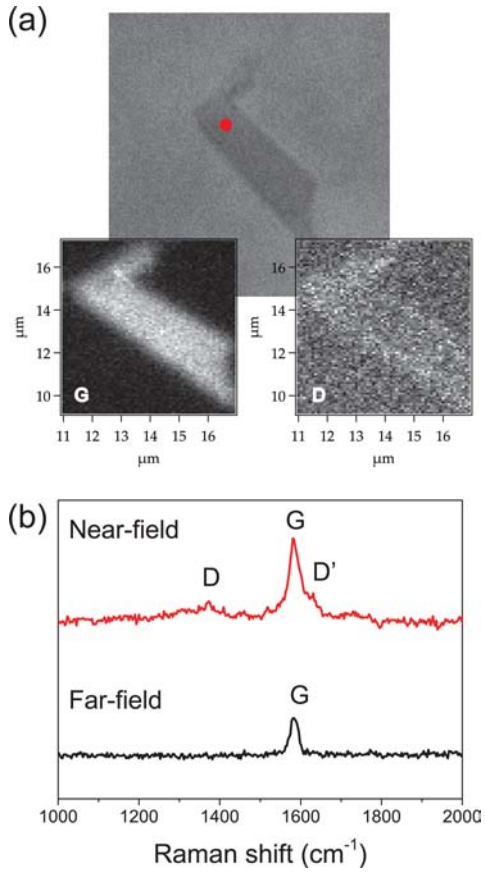

Figure 3. (a) Comparison of topography and G- and D-band nanoimages, which were obtained by TERS spectroscopy with an Ag-coated AFM tip. The mapping of vibrational information was carried out under 532-nm excitation. (b) Comparison of normal Raman (far-field) and TERS (near-field) spectra for the defect-free graphene, measured by changing the tip−sample distance at the red-marked area in the topography.

Here, we focus on elucidating the mechanism of plasmonic activation of the noncenter phonon modes in the absence of defects, from the viewpoint of the selection rules for Raman scattering. When a molecule is exposed to an electromagnetic field, the dipole moment μ in the coordinate of vibration q can be written as

$$\mu_i = [(\partial\mu_{i0}/\partial q)_0 + (\partial\alpha_{ij}/\partial q)_0 E_j + (\partial E_j/\partial q)_0 \alpha_{ij} + 1/3(\partial\beta_{ijk}/\partial q)_0 \nabla_j \cdot E_k]_q$$

where μ_0 is the permanent dipole moment, α and β are the polarizability tensors, and E is the electric field.[8] The first and second terms result in IR absorption and Raman scattering, respectively. The third and fourth terms correspond to the contribution of field gradients to Raman scattering. In the present system, the field gradient is controlled through the dimer gap, d. Thus, the third term is negligible because d of ∼1 nm is still larger than the vibrational displacement of carbon atoms in the graphene lattice. According to group theory, G- and D-phonons are classified as Γ-E_{2g} (D_{6h}) and K-A'_1(D_{3h}) modes, respectively.[23] The corresponding unit cells of these modes are illustrated in Figure 4a. Due to the translational symmetry of the graphene lattice, the second term is responsible only for activation of the G-mode under the dipole approximation. On the other hand, the fourth term can activate the D-mode when the field variations are large enough. Indeed, the smallest gap size in the present experiments is comparable with the unit cell of the D-phonon. Moreover, the β tensor for the D-mode with A'_1 symmetry has a nonzero element of $\beta_{xxx} - 3\beta_{xxy}$, where x and y correspond to the in-plane directions of graphene. This is consistent with the difference in the D-band intensity between Figures 2 and 3; the lateral polarization on the dimer array system can strongly induce the D-band, in

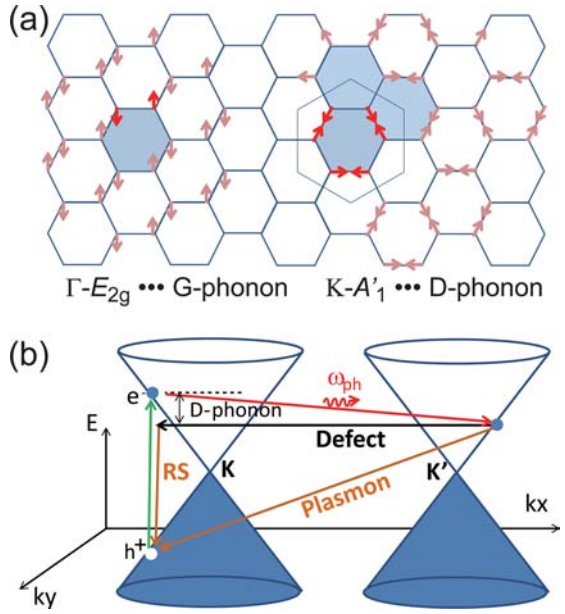

Figure 4. (a) Schematic illustration of the lattice displacements for the G-phonon with Γ-E_{2g} symmetry and for the D-phonon with K-A'_1 symmetry. (b) Comparison of the activation process of the D-band between normal (far-field) and plasmonic (near-field) excitation, consisting of excitation and recombination of electron/hole pair accompanied by excitation of one D-phonon. ω_{ph} and RS denote frequency of phonon and Raman scattering, respectively. Momentum conservation is satisfied by the scattering of excited electrons due to defects in normal Raman and by plasmon-induced dipole-forbidden transition.

dx.doi.org/10.1021/ja4056596 | J. Am. Chem. Soc. 2013, 135, 11489−11492

contrast to the longitudinal polarization of the TERS system which does not induce the D-band very much.

Raman scattering from graphene, induced by visible or near-IR light, is actually an electronic resonance scattering process. This is well expressed in k-space as shown in Figure 4b.[20,21] For G-phonons near the Γ point, the electron/G-phonon scattering can be directly detectable by excitation of an electron/hole pair using freely propagating optical waves with small wave vectors k. On the other hand, the electron/D-phonon scattering has an exchanged momentum $q-K$ between two neighboring K points of the Brillouin zone, which is not directly detectable by optical excitation. In the presence of lattice defects in graphene, double resonance mechanism is widely accepted for D-band activation; the momentum difference is compensated by intervalley electron scattering due to defects. In the case of the plasmon-mediated process, however, such a defect-mediated electron scattering is not needed for the momentum conservation, because the nanoconfined light with larger k vectors makes nonvertical optical transition allowed.[24] The largest wavenumber present in the nanoconfined field is characterized by the variation in the field, i.e., $k_{\mathrm{lateral}} \approx \pi/d \approx 10^7$ cm^{-1} in the dimer system. This is comparable with the momentum difference in the D-phonon. For the intravalley D′-phonon, a similar activation process is possible under plasmonic condition. Consequently, these results indicate that the well-controlled gradient fields can modify selection rules for both vibrational and electronic transitions.

In summary, optical transitions involving both phonon scattering and electronic resonances can be tuned by controlling field gradients through plasmonic confinement of optical fields. In nanoscale characterization, the field gradient is an intrinsic issue. Tunability of the field confinement is the key to utilize the field gradient effect in practical microscopy. In the field of photochemistry, moreover, the use of dipole-forbidden transition may extend the design concept of dye molecules to realize an artificial photoenergy conversion system. Plasmonic field manipulation can be a powerful means not only for enhancement of photon−matter interaction efficiency but also for modification of photon−matter interaction pathway.

AUTHOR INFORMATION

Corresponding Author

kikeda@pchem.sci.hokudai.ac.jp

Notes

The authors declare no competing financial interest.

ACKNOWLEDGMENTS

This research was partially supported by Grants-in-Aid for Young Scientists (A) (No. 24681018) and for Exploratory Research (No. 24651126) from JSPS, and World Premier International Research Center (WPI) Initiative on Materials Nanoarchitechtonics from Ministry of Education, Culture, Sports, Science and Technology (MEXT), Japan.

REFERENCES

(1) Barnes, W. L.; Dereux, A.; Ebbesen, T. W. *Nature* **2003**, *424*, 824.
(2) Bharadwaj, P.; Deutsch, B.; Novotny, L. *Adv. Opt. Photon.* **2009**, *1*, 438.
(3) Moskovits, M. *J. Raman Spectrosc.* **2005**, *36*, 485.
(4) Kneipp, K.; Kneipp, H.; Itzkan, I.; Dasari, R. R.; Feld, M. S. *Chem. Rev.* **1999**, *99*, 2957.
(5) Otto, A.; Mrozek, I.; Grabhorn, H.; Akemann, W. *J. Phys.: Condens. Matter* **1992**, *4*, 1143.
(6) Akiyama, T.; Nakada, M.; Terasaki, N.; Yamada, S. *Chem. Commun.* **2006**, 395.
(7) Ikeda, K.; Takahashi, K.; Masuda, T.; Uosaki, K. *Angew. Chem., Int. Ed.* **2011**, *50*, 1280.
(8) Ayars, E. J.; Jahncke, C. L.; Paesler, M. A.; Hallen, H. D. *J. Microsc.* **2001**, *202*, 142.
(9) Sass, J. K.; Neff, H.; Moskovits, M.; Holloway, S. *J. Phys. Chem.* **1981**, *85*, 621.
(10) Zeman, E. J.; Schatz, G. C. *J. Phys. Chem.* **1987**, *91*, 634.
(11) Osawa, M.; Matsuda, N.; Yoshii, K.; Uchida, I. *J. Phys. Chem.* **1994**, *98*, 12702.
(12) Chenal, C.; Birke, R. L.; Lombardi, J. R. *ChemPhysChem* **2008**, *9*, 1617.
(13) Ikeda, K.; Suzuki, S.; Uosaki, K. *Nano Lett.* **2011**, *11*, 1716.
(14) Nordlander, P.; Oubre, C.; Prodan, E.; Li, K.; Stockman, M. I. *Nano Lett.* **2004**, *4*, 899.
(15) Sheikholeslami, S.; Jun, Y.-W.; Jain, P. K.; Alivisatos, A. P. *Nano Lett.* **2010**, *10*, 2655.
(16) Sawai, Y.; Takimoto, B.; Nabika, H.; Ajito, K.; Murakoshi, K. *J. Am. Chem. Soc.* **2007**, *129*, 1658.
(17) Zuloaga, J.; Prodan, E.; Nordlander, P. *Nano Lett.* **2009**, *9*, 887.
(18) Romero, I.; Aizpurua, J.; Bryant, G. W.; García de Abajo, F. J. *Opt. Exp.* **2006**, *14*, 9988.
(19) Rao, C. N. R.; Sood, A. K.; Subrahmanyam, K. S.; Govindaraj, A. *Angew. Chem., Int. Ed.* **2009**, *48*, 7752.
(20) Saito, R.; Jorio, A.; Souza Filho, A. G.; Dresselhaus, D.; Dresselhaus, M. S.; Pimenta, M. A. *Phys. Rev. Lett.* **2002**, *88*, 027401.
(21) Pimenta, M. A.; Dresselhaus, G.; Dresselhaus, M. S.; Cançado, L. G.; Jorio, A.; Saito, R. *Phys. Chem. Chem. Phys.* **2007**, *9*, 1276.
(22) Hayazawa, N.; Yano, T.; Kawata, S. *J. Raman Spectrosc.* **2012**, *43*, 1177.
(23) Malard, L. M.; Guimarães, M. H. D.; Mafra, D. L.; Mazzoni, M. S. C.; Jorio, A. *Phys. Rev. B* **2009**, *79*, 125426.
(24) Beversluis, M. R.; Bouhelier, A.; Novotny, L. *Phys. Rev. B* **2003**, *68*, 115433.